Astronomical and Astrophysical Transactions (*AApTr*), 2022, Vol. 33, Issue 3, pp. 297–312,
ISSN 1055-6796, Photocopying permitted by license only, ©Cambridge Scientific Publishers

Dark matter fermions: from linear to non-linear structure formation

C.R. Argüelles[1,2,*], E.A. Becerra-Vergara[1,3,4], V. Crespi[2], A. Krut[1], J.A. Rueda[1,3,5], R. Ruffini[1,3,5,6], R.I. Yunis[1,3]

[1]*International Center for Relativistic Astrophysics Network – ICRANet, Piazza della Repubblica 10, 65122 Pescara, Italy*
[2]*Instituto de Astrofísica de La Plata (CONICET, UNLP), Paseo del Bosque, B1900FWA La Plata, Argentina*
[3]*ICRA, Dipartimento di Fisica, Sapienza Università di Roma, Piazzale Aldo Moro 5, 00185 Rome, Italy*
[4]*GIRG, Escuela de Física, Universidad Industrial de Santander, 680002, Cra 27 calle 9, Bucaramanga, Colombia*
[5]*ICRANet-Ferrara, Dip. di Fisica e Scienze della Terra, UNIFE, Via Saragat 1, 44122 Ferrara, Italy*
[6]*INAF, Istituto de Astrofisica e Planetologia Spaziali, Via Fosso del Cavaliere 100, 00133 Rome, Italy*

Received 14 December, 2022

The transition from linear to non-linear structure formation in cosmology is here studied from the point of view of the thermodynamics of self-gravitating fermions. We start by reviewing the principle of maximum entropy production through which such a fermionic system can relax towards spherical equilibrium states able to explain the dark matter (DM) in galaxies. We then analyze the stability, lifetime and morphology of the above configurations, and show that the most general DM profile develops a compact core governed by degeneracy pressure, which is surrounded by an extended halo. For DM particles which are in the range of $\mathcal{O}$(10–100) keV, we apply this theory to the case of the Milky Way, and show that the compact DM-core explains the dynamics of all the best resolved S-cluster stars orbiting SgrA *, without the need of assuming a central black hole (BH). Further consequences of this theory regarding open issues in cosmology are outlined, including the problem of formation of supermassive BHs in the early Universe.

Keywords: Dark matter – Galaxy dark matter halos – Milky Way dark matter halo – thermodynamics of self-gravitating systems – gravitational collapse – supermassive black holes

*Email: carguelles@fcaglp.unlp.edu.ar

1 Introduction

In the particle DM paradigm, diverse particle candidates (e.g. WIMPS, axions, sterile neutrinos, etc.) have different early Universe histories. This, in turn, translates into a different evolution of the primordial perturbations in the cosmic plasma that serve as seed for galaxy formation at later stages [1]. In most cases, the effects of the DM microphysics is quantified only by the linear matter power spectrum that measures the distribution of density perturbations prior to the onset of non-linear processes. A prime example of these processes is the gravitational collapse of primordial DM seeds, required for the formation of the observed structures in the late Universe, such as galaxies and clusters.

Traditionally, numerical simulations for structure formation involve the quantum nature of the DM particles only in the initial conditions, and before the action of self-gravity. Hence, the explicit role of the possible DM nature (i.e. bosonic or fermionic) in the dynamics of the formed systems is neglected, since the building blocks at the basis of the simulations are classical pseudo-particles.

The (intrinsic) limited spatial resolution of DM halos in cosmological N-body simulations implies huge uncertainties on the DM central distribution. This issue leaves room for open questions, such as i) How does DM correlate with the baryonic matter at such inner scales? ii) Is it related to supermassive black holes (SMBH) harbored at the center of large galaxies? iii) How can they co-exist in a steady state? The use of classical point-like masses as the constituents of matter (without considering the quantum nature of the particles) in traditional N-body simulations within the ΛCDM paradigm does not allow for any source of quantum pressure (as recently shown within 3D numerical simulations for bosons [2] or fermions [3]. The existence of quantum effects at the center of equilibrium systems of self-gravitating quantum particles is a long-known physical phenomenon [4].

Motivated by these open issues, we will show how an alternative mechanism of structure formation in cosmology – in which the quantum nature of the fermions is taken into account within a principle of entropy maximization – opens the possibility to describe the behavior of the DM distribution from center to periphery, with key implications to DM halo stability; SMBH formation; the nature and mass for the DM particles; and also allows to address different tensions existing in ΛCDM or ΛWDM cosmologies.

2 The formation of DM halos: a thermodynamic approach

Motivated by the seminal work of Lynden-Bell on violent relaxation [5], we perform a thermodynamic approach for the formation of DM halos. Relevant extensions to Lynden-Bell theory allowing for out-of-equilibrium effects (i.e. particle evaporation), were performed by [6, 7] using the framework of kinetic theory. Quasi-stationary solutions to such equations (see Eq. 2 below) lead to the most-probable, coarse-grained distribution function (DF) at (violent) relaxation. This DF allows more realistic applications than the original Lynden-Bell's version, and is mathematically

described by a tidally truncated Fermi–Dirac DF

$$\bar{f}(\epsilon \leq \epsilon_c) = \frac{1 - e^{(\epsilon-\epsilon_c)/kT}}{e^{(\epsilon-\mu)/kT} + 1}, \qquad \bar{f}(\epsilon > \epsilon_c) = 0\,, \tag{1}$$

where $\epsilon = \sqrt{c^2p^2 + m^2c^4} - mc^2$ is the particle kinetic energy, μ is the chemical potential with the particle rest-energy subtracted off, T is the effective temperature, k is the Boltzmann constant, c is the speed of light, and m is the DM fermion mass. The full set of dimensionless parameters of the model are defined by the temperature, degeneracy and cutoff parameters, respectively $\beta = kT/(mc^2)$, $\theta = \mu/(kT)$ and $W = \epsilon_c/(kT)$. The subscript 0 will be used when the parameters are evaluated at the center of the configuration.

In the limiting case of $\epsilon_c \gg \epsilon$, there is no particle escape and (1) reduces to the traditional Fermi–Dirac DF obtained in the original work of Lynden-Bell. This DF is a stationary solution of the Vlasov–Poisson (VP) equation governing collisionless systems [6], namely a solution of Eq. (2) shown below, with $\mathbf{J} = 0$, usually called 'VP dynamically-stable' solutions. The more realistic "tidally-truncated" DF (1) is another kind of quasi-stationary solution of the more general *convection–diffusion* kinetic equation (2), as demonstrated in [6, 8]. This accounts for the 'microphysics' of the long-range particle–particle interactions[1] involved in the diffusion current $\mathbf{J}$, caused mainly by the rapid fluctuations of the gravitational potential (proper of violent relaxation processes):

$$\frac{\partial \bar{f}}{\partial t} + \mathbf{v}\frac{\partial \bar{f}}{\partial \mathbf{r}} - \nabla\Phi\frac{\partial \bar{f}}{\partial \mathbf{v}} = -\frac{\partial \mathbf{J}}{\partial \mathbf{v}}. \tag{2}$$

At the end of relaxation, when the gravitational fluctuations die, the diffusion current approaches zero (i.e. no more evaporation), and the DF (1) remains as a stationary solution of the VP equation. These dynamically-stable VP solutions can be used to build DM halos in hydrostatic equilibrium and to reproduce galaxy rotation curves (as shown in [9, 10]). However, such analysis does not elucidate how the collisionless self-gravitating systems reach the required steady state, or if the halos maximize the coarse-grained entropy S of the fermion-gas, or if they are just transitory (unstable/unreachable) states. This is due to the fact that VP dynamical stability *does not* necessarily imply thermodynamical stability. Therefore, some dynamically stable solutions for DM halos in hydrostatic equilibrium can be more likely to occur in nature than others.

As we shall show in this article (see also details in [3]), the DM halos built upon the fermionic DF (1) in a cosmological framework are naturally finite-sized, can be stable and extremely long-lived, and imply a mechanism for the formation of supermassive BHs at the center of massive galaxies.

In order to find dynamically and thermodynamically stable configurations of collisionless self-gravitating fermions in general relativity (GR), capable of modeling realistic DM halos, it is necessary to solve the problem of finding solutions that maximize the global entropy $S = \int_0^R s(r)e^{\lambda/2}4\pi r^2 \mathrm{d}r$ (at fixed total energy and particle

[1]For isolated systems made of fermions, such a current can make (2) to be of the form of a fermionic Landau equation, conserving mass and energy, and continuously increase the Fermi–Dirac entropy functional (i.e. fulfilling H-theorem) [8].

number), where $s(r)$ is the entropy density given by the Gibbs–Duhem relation

$$s(r) = \frac{P(r) + \rho(r) - \mu(r)n(r)}{T(r)}, \tag{3}$$

$e^{\lambda/2}4\pi r^2 dr$ is the proper volume, being e^{λ} the spatial component of the spherically-symmetric space–time metric: $\mathrm{d}s^2 = e^{\nu}c^2\mathrm{d}t^2 - e^{\lambda}\mathrm{d}r^2 - r^2\mathrm{d}\Theta^2 - r^2\sin^2\Theta\mathrm{d}\phi^2$, with (r, Θ, ϕ) the spherical coordinates, and ν and λ depend on r.

The mass–energy density $\rho(r)$, pressure $P(r)$ and particle number density $n(r)$ are directly obtained as the corresponding integrals of $\bar{f}(p)$ over momentum space (until the $\epsilon \leq \epsilon_c$) as detailed in [3]. This leads to a four-parametric equation of state $(\rho(r), P(r))$ depending on (β, θ, W, m) according to the dimensionless parameters in (1). In agreement with the isotropy of the phase-space, we use the stress–energy tensor of a perfect fluid with the above density and pressure. Therefore, the self-gravitating configurations of fermions are solutions of the hydrostatic equilibrium equation, with the local $T(r)$ and $\mu(r)$ fulfilling, respectively, the Tolman and Klein equilibrium relations (see [3] for details). We shall analyze which of such solutions are thermodynamically stable and of astrophysical interest regarding realistic DM halos in cosmology.

The stability analysis can be solved using the 'Katz criterion' [11] that allows us to find the full set of thermodynamically-stable solutions (i.e., maxima of global entropy S) along the full series of equilibrium solutions of self-gravitating fermions. This method relies only upon the derivatives of the caloric curve given by total energy $E = c^2M(R)$ vs. $1/T_\infty$ (like in Figure 1), without the need of calculating the second order entropy variations $\delta^2 S$. This method is commonly used to calculate the stability of self-gravitating systems (see, e.g., [8, 3]). We work in the microcanonical ensemble which is the most appropriate for astrophysical applications (see [8] for details). The relevant thermodynamic potential to be extremized in this ensemble is the coarse-grained entropy S.

In order for such a maximization entropy problem to be well defined, the self-gravitating solutions with given particle number $N = \int_0^R n(r)e^{\lambda/2}4\pi r^2\mathrm{d}r$ and total energy $E = c^2M(R)$ must be bounded in radius, as occurring when working with the tidally-truncated DF (1). Therefore, our approach is well posed and does not need to impose unrealistic bounding boxes [3].

3 Cosmological and astrophysical applications

We use the following technique to assure that the fixed boundary conditions (N and the corresponding $M(R)$ required to maximize the global entropy S) correspond to values of a given fermionic halo in a realistic cosmological framework. **(i)** We calculate the linear matter power spectrum for the fermionic (quantum) candidates; **(ii)** We apply the corresponding Press–Schechter formalism to obtain the virial halo mass, $M_{\rm vir} \equiv M(R \equiv R_{\rm vir})$, with associated redshift $z_{\rm vir}$ for such a particle mass; **(iii)** We use the most probable coarse-grained DF (1) obtained at the end of violent relaxation (valid for that redshift), to obtain the full families of DM (equilibrium) profiles in agreement with the above virial constraints. Once done, we can use the

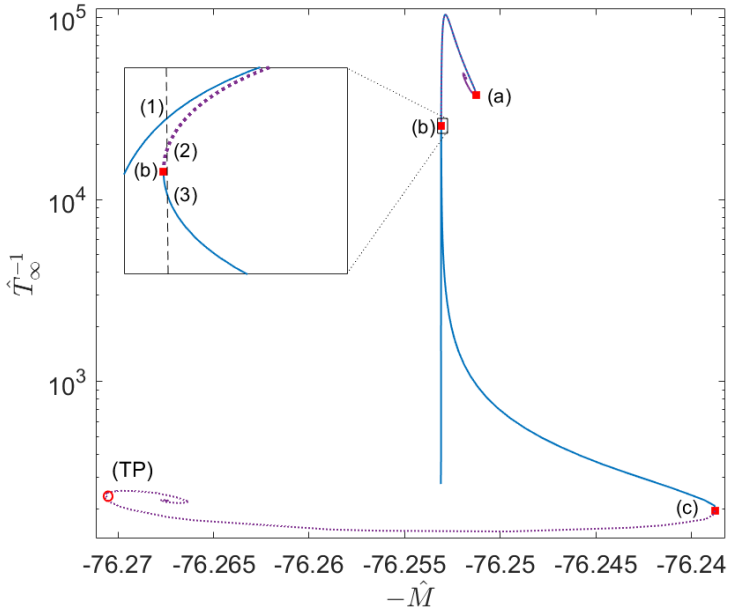


Figure 1 Series of equilibrium solutions along the caloric curve for tidally-truncated configurations of $mc^2 = 48$ keV fermions, for typical DM halos of $M_{\rm vir} \approx 5 \times 10^{10} M_\odot$. According to the Katz criterion, the equilibrium states within the continuous-blue branches are thermodynamically (and dynamically) stable, while the dotted-violet branches – between (a) and (b) and after (c) – are unstable. Figure extracted from [3].

Katz criterion to analyze the (thermodynamic) stability of such halos in a given cosmological framework, and further test their astrophysical applications.

This strategy was recently applied in [3] within a WDM cosmology for fermion masses of $\mathcal{O}(10)$ keV, and illustrated here for an average DM halo of mass $M_{\rm vir} \approx 5 \times 10^{10} M_\odot$, which started to form at $z_{\rm vir} \approx 10$ according to the Press–Schechter formalism in our cosmological setup.

We show in Figure 1 the caloric curve in dimensionless variables, $-\hat{M}$ vs. $1/\hat{T}_\infty$, for a DM halo (with corresponding $\hat{N} = 76.25$, and $W_0 - \theta_0 = 24$ typical of average-size galaxies [3]), in the case of fermions of mass $mc^2 = 48$ keV. The stability analysis follows the procedure **(i–iii)** mentioned above. A simple way to understand how the Katz criterion operates is: (a) an unstable mode arises when the caloric curve *rotates clockwise* (i.e. when the negative slope in the $(-\hat{M},\ \hat{T}_\infty^{-1})$ curve becomes infinite for then turning into positive), (b) when the same curve *rotates counterclockwise* a stable mode has been re-gained (the latter implying that a positive slope turned into negative just after becoming vertical). In this sense, once in a given unstable branch of the caloric curve, it is necessary as many counterclockwise turns of the curve as clockwise passed, to regain the thermodynamic stability (see Appendix A in [3] for details).

In Figure 1, we display the full family of thermodynamically stable (i.e. maxima of S) solutions (continuous-blue curve) and the thermodynamically unstable (i.e., minimum or saddle points of S, dotted-violet curve). There are two spiral features in this

caloric curve. The upper spiral arises due to the fermion (quantum) degeneracy which avoids the so-called *gravothermal catastrophe* typical of Boltzmannian distributions (as first shown for classical systems in [12]). The second spiral has relativistic origin and leads to the turning point criterion for gravitational collapse discussed below.

In the next three subsections, we highlight the principal findings of this stability analysis, and its cosmological and astrophysical implications.

3.1 The structure of fermionic DM halos

From the caloric curve of Figure 1 we analyze all the possible outcomes of density profiles for a conveniently fixed value of the total energy $\hat{M}$ (see vertical black-dashed line in the inset-box of Figure 1, leading to the associated profiles of Figure 2). There exist two different families of stable DM profiles (astrophysical) in a $\mathcal{O}(10)$ keV cosmology, arising from our thermodynamic halo-formation approach. They are either King-like, as the solution (1) in Figure 2 (resembling the Burkert profile), or they develop a *core-halo* morphology, like the solution (3) in Figure 2. Both kinds of solutions agree with the observational DM surface density relation of galaxies (the latter $\propto \rho(r_{pl})\, r_h$, with $\rho(r_{pl})$ the density at plateau, and r_h the one-halo scale-length of such profiles), as demonstrated in [3]. In the case of King-like profiles, the fermions are in a dilute regime (i.e., $\theta_0 \ll -1$) and correspond to a global maxima of entropy. In the case of a *core-halo* distribution, the degeneracy pressure (i.e. Pauli principle) is holding the quantum core against gravity, and corresponds to a local maxima of entropy. This

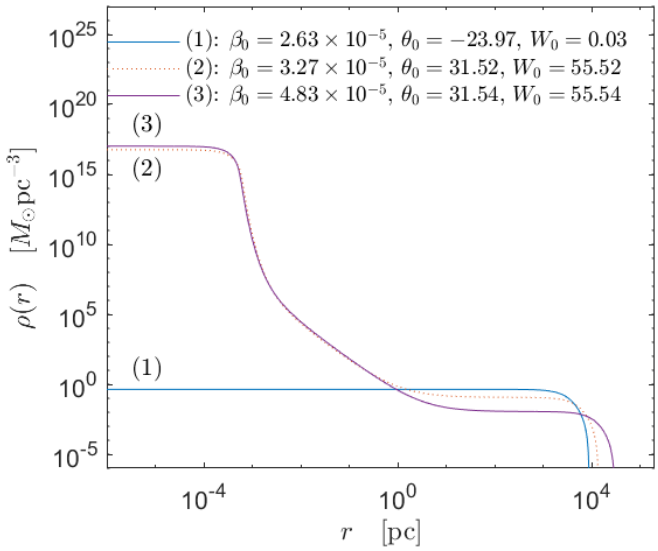


Figure 2 Density profiles for $mc^2 = 48$ keV corresponding with three different solutions along the caloric curve in Figure 1 at a fixed energy. Only the profiles (1) (resembling a King distribution) and the *core-halo* one (3) are stable, while profile (2) is thermodynamically unstable. Solutions like (3) successfully explain the Milky Way rotation curve (see Figure 4). They are stable, extremely long-lived and fulfill with different observational probes. Figure extracted from [3].

kind of fermionic *core-halo* solutions are usually referred to as the Ruffini–Argüelles–Rueda (RAR) model [13, 9]. These are extremely long-lived, meta-stable states as demonstrated in [3], with a lifetime $\propto e^N$, and more likely to arise in Nature than the former as argued in [8].

The present thermodynamic approach for DM halo formation also implies that, on inner scales, the $\mathcal{O}(10)$ keV fermionic density profiles develop an extended plateau (similar to Burkert profiles, with or without the innermost quantum core depending on the degree of central degeneracy), thus not suffering from the core-cusp problem associated with the ΛCDM cosmology [14]. While N-body simulations (within the CDM paradigm) obtain 'cored' profiles by including DM self-interactions (see e.g. [15]), here the flatness on inner halo scales arise due to the fulfillment of an entropy maximization. The latter can be achieved thanks to the long range particle–particle interactions involved in the diffusion-current term of equation (2) (see also footnote 1), and could be also enhanced by (short-range) DM self-interactions.

3.2 Gravitational core-collapse of DM and SMBH formation

The approach considered in this work regarding DM halos formation also predicts a novel SMBH formation mechanism from DM. A galactic quantum DM core, like solution (3) of Figure 2, might become so densely packed that, above a threshold critical mass, the quantum pressure can no longer support its own weight, leading to the gravitational collapse of the core with consequent formation of a SMBH. The threshold solution corresponds to the last stable configuration depicted by point (c) in the caloric curve of Figure 1, below which there is no possible accessible state (see [3] for details). This collapse occurs *prior* to the turning point in the (traditional) *total mass* vs. *central density* diagram (see Figure 3).

The DM core-collapse occurs only when the total particle number exceeds the so-called Oppenheimer–Volkoff limit (i.e., when $\hat{N} > \hat{N}_{\rm OV} \approx 0.4$, as fulfilled in the case here exemplified of $\hat{N} = 76.25$). However, a stable branch of *core-halo* solutions can also exist, for which $\hat{N} > \hat{N}_{\rm OV}$ as exemplified through the solution (3) in Figure 1, before the last stable one (c). This fact is characteristic of self-gravitating solutions of fermions at finite T (as in the RAR model), which differ from the traditional $T \to 0$ limit where the system must necessarily collapse when $\hat{N} > \hat{N}_{\rm OV}$ (see [3] for further details).

At the center of a realistic DM halo with $mc^2 \approx 50$ keV, is possible to form a SMBH of $M_c^{\rm cr} \approx 2 \times 10^8 M_\odot$ for $\hat{N} > \hat{N}_{\rm OV}$. This is the last stable configuration at the onset of collapse of the core, i.e., point (c) in Figure 1) correspond to a critical core mass $M_c^{\rm cr} = 2.17 \times 10^8 M_\odot$, and thus its collapse forms SMBH of this mass (see [3] for further details). This is an interesting number, since $\sim 10^8 M_\odot$ appears to be a value that distinguishes between the mass of the central object in active and non-active galaxies [16]. In this scenario, the massive central objects in non-active galaxies are DM dense cores, while in active galaxies SMBHs form from DM core-collapse. The DM core-collapse scenario can occur within the high $z \sim 10$ Universe when such halos start to form, without the need of prior star formation or any BH seed mechanisms involving (likely unrealistic) super-Eddington accretion rates. This may provide the long-sought solution to the problem of SMBH formation in the early Universe, which deserves further detailed investigations.

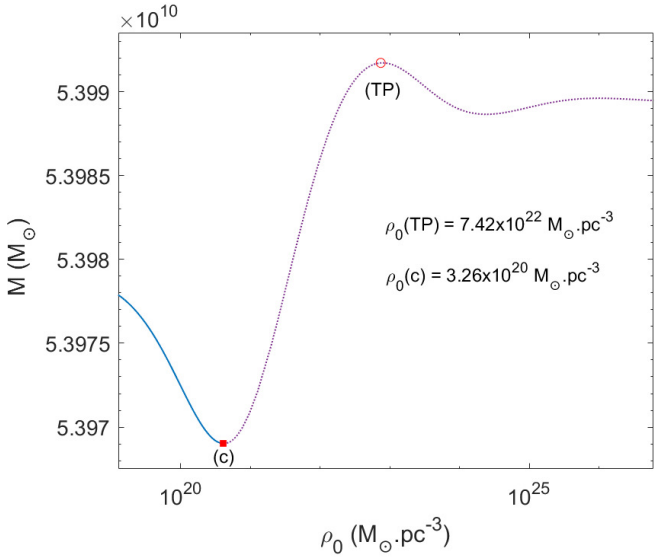


Figure 3 Series of equilibrium states with $N > N_{\rm OV}$ are shown along a ρ_0 vs. M curve, in correspondence with the caloric curve of Figure 1. The last stable configuration at the onset of core-collapse occurs at the minimum of this curve and *prior* to the turning point instability (corresponding with point (c) in Figure 1). Such a solution has a critical core mass $M_c^{\rm cr} \approx 2 \times 10^8 M_\odot$, thus allowing the formation of a SMBH from DM core-collapse. Figure extracted from [3].

We can express the critical value triggering core-collapse in a more familiar way, in terms of the Planck mass m_{pl} and the fermion mass m as $N_{\rm OV} \approx 0.398\, m_{pl}^3/m^3$, corresponding to a critical (total) mass $M_{\rm OV} \approx 0.384\, m_{pl}^3/m^2$ which for $m \approx 50$ keV yields $M_{\rm OV} \sim 10^8 M_\odot$. Therefore, equilibrium configurations of fermions at finite T_∞ with $M_{\rm vir} < 10^8 M_\odot$ can not undergo core-collapse towards a SMBH within the present scenario. Indeed, the caloric curves in these cases never develop a last stable solution, like (c) in Figure 1, nor the second spiral of relativistic origin as shown in [3].

The above numbers imply that the critical mass for gravitational collapse can not be reached for smaller DM halos, for example those surrounding typical dwarf galaxies with $M_{\rm vir} \lesssim 10^8 M_\odot$. Instead, this $\hat{N} < \hat{N}_{\rm OV}$ scenario would leave smaller dwarf galaxies with a central DM core with a mass typically of $M_c \sim 10^5 M_\odot$ (or less) as shown in [10]. This provides an explanation of the existence of the so-called 'intermediate-mass BHs'. These DM cores can still mimic the gravitational signatures of a central BH, whilst the DM outer halo can explain the observed galaxy rotation curves [10] as well.

3.3 The case of the S star-cluster

The compact object at the center of our galaxy, SgrA*, is surrounded by a small stellar cluster known as the S-Cluster. It contains stars that are closest to the galactic center

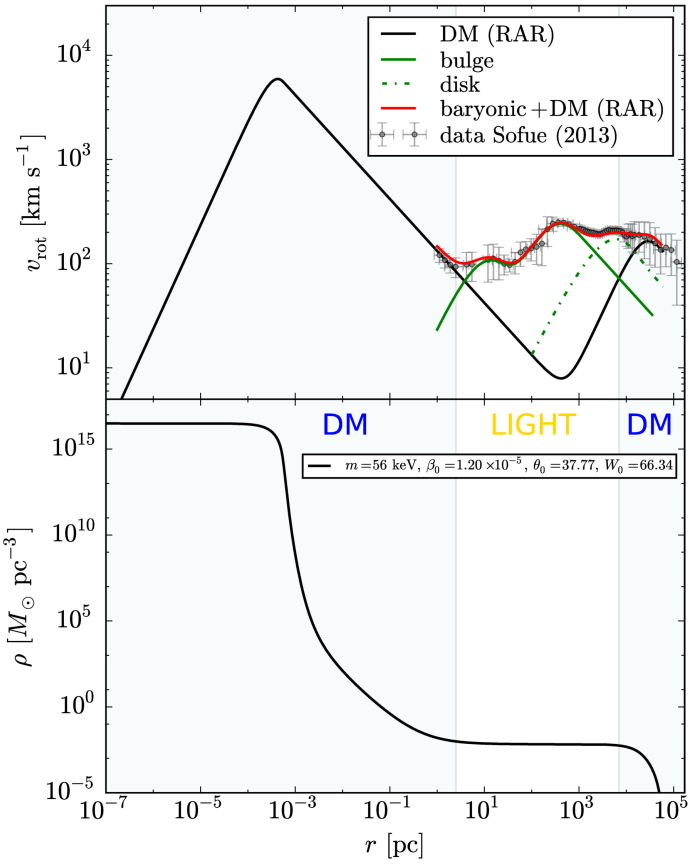


Figure 4 Top: Milky Way rotation curve $v_{\rm rot}$ (red), contributions of DM (black) and baryonic (bulge + disk) components (green). Bottom: corresponding core-halo DM RAR profile for $mc^2 = 56$ keV with a DM quantum core of mass of $M_c = M(r_c) = 3.5 \times 10^6 M_\odot$. Figure extracted from [17].

(within an arcsecond of angular distance), and they provide a very important tool to trace the gravitational potential in which they move.

As mentioned before, the rotation curves of galaxies can be explained by configurations like solution (3) in Figure 2, in particular for the Milky Way (see Figure 4), while the dense quantum core can work as an alternative to the SMBH in non-active galaxies [9, 10, 17, 18]. A deeper analysis in the case of the Milky Way was made in [17] within the extended RAR model for $mc^2 = 56$ keV. There, it has been shown that the gravitational potential of the DM dense core leads to a better fit of the orbits of the S2 and G2 objects around SgrA*, with respect to the one obtained by the central BH model (see Figures 5 for the case of S2 as an example). Moreover, the extended RAR model naturally predicts the geodesic of the G2 object in the gravitational field of the DM profile [17], that is, the post-pericenter slowing down phenomenon as observed in [19]. This solution contrasts with the BH model within which the slowing down of G2 has been explained by introducing a drag force caused by an accretion flow onto

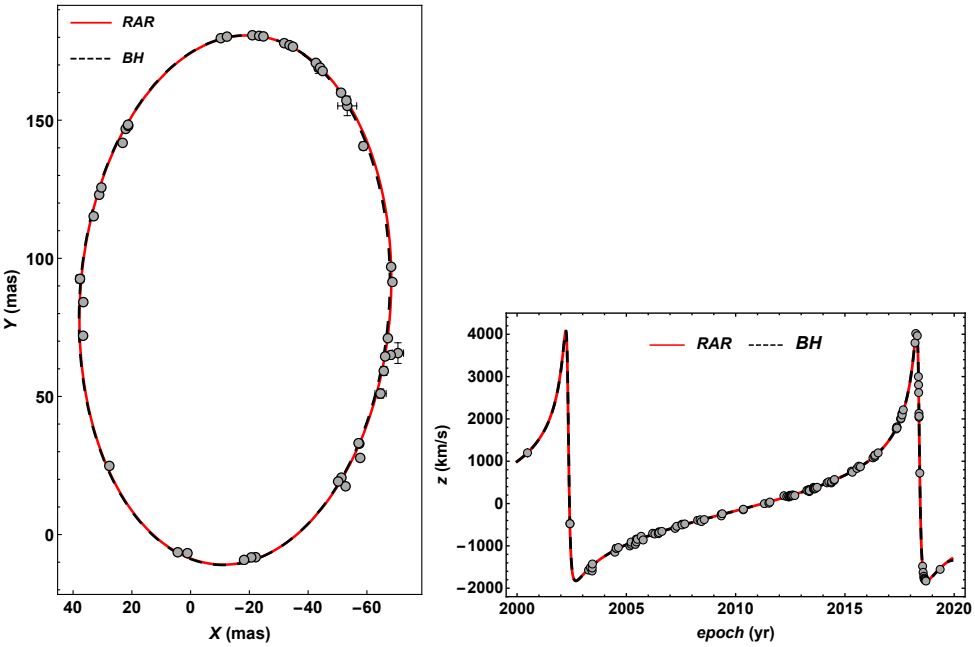


Figure 5 Theoretical and observed orbit and radial velocity (z) of S2 around Sgr A* (with data taken from Ref. [23]). Top panel: shows the projected orbit on the sky, X (Right Ascension) vs. Y (Declination). Bottom panel: shows the line-of-sight radial velocity as a function of time. The theoretical models are calculated by solving the equations of motion of a test particle in the gravitational field of: (i) a Schwarzschild BH of $4.075 \times 10^6\ M_\odot$ (*black dashed curve*), and (ii) the fermionic DM distribution obtained from the core-halo RAR model with $mc^2 = 56$ keV fermions (*red curves*). Figure adapted from Ref. [17].

the massive BH [20, 19]. The possibility of the DM nature of Sgr A* strengthens with the results of [18], in which the up-to-date astrometry data of the dynamics of the 17 best-resolved S-stars orbiting Sgr A* is explained with similar (and some cases better) accuracy as compared to a central BH model.

4 Precession of the S2 star

In this section we study exclusively the S2 star. It has a period of about 16 yr and an approximate pericenter of 1450 Schwarzschild radii for the $4 \times 10^6 M_\odot$ central object. It shows one of the most compact orbits around SgrA* and the amount of astrometric data collected dates over 27 years, being its most precise data taken around pericenter passages [21, 22, 23].

With two alternative scenarios in mind: i) different configurations of the RAR extended model and ii) a Schwarzschild BH model, we analyze here the relativistic pericenter precession of the S2 star. In both cases the metric of the spherically symmetric space-times can be written as $ds^2 = g_{00}(r)c^2dt^2 - g_{11}(r)dr^2 - r^2(d\theta^2 + sin^2(\theta)d\phi^2)$, where (r, θ, ϕ) are the spherical coordinates, c is the speed of light,

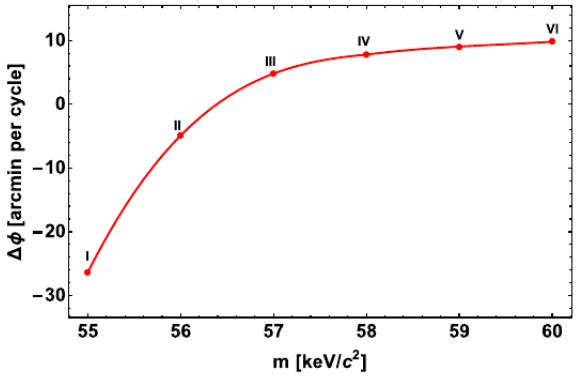


Figure 6 Relativistic pericenter precession $\Delta\phi_{DM}$ per cycle as a function of the darkino mass predicted by the RAR DM models for the S2-star. The precession is retrograde for $m < 56.4$ keV while it becomes prograde for $m > 56.4$ keV.

and $g_{00}(r)$, $g_{11}(r)$ are the metric functions to be found by solving the Einstein field equations. The geodesic of a test particle in these spaces can be simplified as

$$\begin{cases} \dot{t} = \dfrac{E}{c^2 g_{11}(r)} \\ \dot{\phi} = \dfrac{L}{r^2} \\ \ddot{r} = \dfrac{1}{2g_{00}(r)} \left[-g'_{11}(r)c^2\dot{t}^2 - g'_{00}(r)\dot{r}^2 + 2r\dot{\phi}^2 \right], \end{cases} \tag{4}$$

where E and L are the conserved energy and angular momentum of the test particle per unit mass, the overdot stands for derivatives with respect to the proper time τ, while the superscript $(')$ denotes derivatives with respect to the radial coordinate r. We perform the numerical integration of the geodesic with appropriate initial conditions chosen such that the test particle motion starts at the apocenter $[t(\tau_0), \phi(\tau_0), r(\tau_0), \dot{r}(\tau_0)] = [0, \pi, r_a, 0]$. With two consecutive cycles we can compute the net precession of the real orbit, denoting the respective times of apocenter as t_{apo1} and t_{apo2} the precession of the real orbit over those 2 cycles is $\Delta\phi_{DM} = |\phi(t_{apo2}) - \phi(t_{apo1})| - 2\pi$. In the BH case, the value of the precession angle per cycle is given by the well known expression $\Delta\phi_{BH} = 6\pi GM_{BH}/[c^2 a(1-e^2)]$, which has the particularity that is always prograde ($\Delta\phi_{BH} > 0$) and for a $4.07 \times 10^6 M_\odot$ BH mass and the S2 orbital parameters gives ~ 12 arcmin per cycle (further details in [24]).

Using the publicly available astrometric measurements from [23] that include data obtained from the instruments NIRC on Keck I (1995–2005) and NIRC2 on Keck II (2005–2018), we analyze the effects of different DM configurations in a small range of darkino masses (from 55 keV to 60 keV) on the value of the angle precession as defined above for the S2 star. As the main result of this analysis, the precession of the S2 star predicted by the extended RAR DM model can be either retrograde or prograde, depending on the amount of DM mass enclosed within the orbit. In Figure 6 we show the angle precession as a function of the darkino mass. It has a non-linear growth

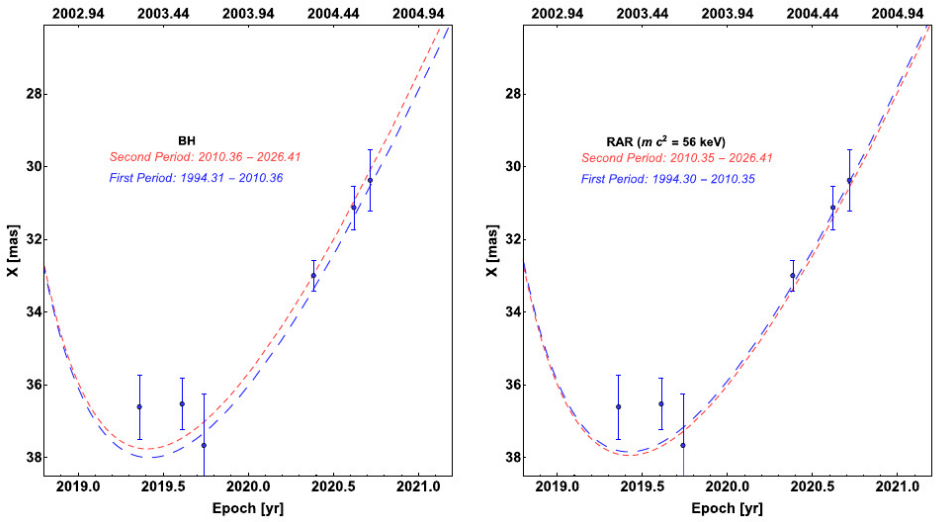


Figure 7 Relativistic precession of S2 for two consecutive periods displayed in right ascension for a BH model (left panel) and for a RAR model with darkino mass of $m = 56$ keV (right panel).

from negative to positive values (i.e. from retrograde to prograde precession) with the darkino mass. Given the morphology of these DM configurations, the two possible outcomes for the angle precession can be explained qualitatively by two overall effects: i) a prograde effect caused by the gravitational potential of the DM core totally inside the S2 pericenter (assimilating to a relativistic point-like source) and ii) a retrograde effect caused by the gravitational potential generated by the extended mass between the pericenter and the apocenter given by

$$\Delta M_{DM} = \int_{r_p}^{r_a} 4\pi r^2 \rho_{DM}(r) dr. \tag{5}$$

Both effects are related to each other, i.e. the larger the darkino mass, the more compact and denser the DM core is (resembling more and more the BH case; [9], with consequent less extended mass fraction $\Delta M_{DM}/M_c$ (where M_c is the mass of the central core), leading to an increasingly positive value for the precession angle until it tends to the one predicted by the BH model.

In order to compare the predictions for the pericenter precession of both models with the astrometric data, we calculate the orbit of the S2 star in the plane of the sky (see Figure 5) and the corresponding precession $\Delta\phi_{sky}$. The best-fitting orbital parameters were obtained following the procedure of [17] for the S2 star, with DM mass of $m = 56$ keV.

In Figure 7 we show the S2 orbit precession effects in right ascension (X) as a function of time, predicted by each of the above two models. A clear difference in X can be seen between two consecutive periods, each one starting at about pericenter passage and extending beyond it, where the predicted precession in each model is most evident. Indeed, near next apocenter passage in 2026 the shifts in X will be maximal for both models ($\Delta X_{BH} \cong 0.7$ mas and $\Delta X_{DM} \cong 0.3$ mas, see [24]). Unfortunately,

the publicly available data in the relevant time window of Figure 7 are only a few data points within the first period (shown in blue dots and obtained from [23]), where the large error bars impede to discriminate between prograde or retrograde precession.

5 Conclusions

A mechanism of DM halo formation based on a principle of entropy maximization which accounts for the (fermionic) quantum nature of the particles, may answer crucial open questions in cosmology. In particular, it allows us to (i) constrain the mass of the DM particles in the keV range; (ii) provide a novel mechanism of SMBH formation from DM core-collapse; (iii) offer a possible understanding of the nature of intermediate mass BHs in small halos; and (iv) offer a solution to the *core-cusp* problem. Furthermore, the particular morphology of these DM configurations, namely *core-halo*, allows for a more general picture over one of the predictions of Einstein's General Relativity, the relativistic precession effect. Unlike the classical case of a Schwarzschild BH, these DM configurations predict not only prograde precession but retrograde precession as well. The value of the precession angle is strongly dependent on the mass of the DM particles, which determines the compactness of the central core and consequently the amount of DM mass that fills the orbit from pericenter to apocenter of the star. With increasing DM particles mass, the value of the precession angle growth from negative to positive values tending to the one predicted by the BH model with mass of $4.07 \times 10^6 M_\odot$ as for Sgr A*. When applied to the S2 star, with the currently public astrometric data we can not distinguish between prograde or retrograde precession. Hopefully, with the upcoming data close to the next apocenter passage in 2026, we will have a good opportunity to confirm one of the predicted directions of the orbital precession.

Studying additional stars of the S-Cluster, such as S62 and S4714, may help us to further constrain the range of the DM particle masses.

Interestingly, the mass and nature of the DM particles involved in the linear matter power spectrum calculations (obtained in [3] within a CLASS code for a WDM cosmology of $\mathcal{O}(10)$ keV), are the same building blocks at the basis of the virialized DM configurations with its inherent effects in the *core-halo* profiles. For the fermion masses currently studied, these DM halos produce the same ΛCDM power-spectrum on scales extending up to $\mathcal{O}$(Mpc), hence providing the expected large-scale structure (see Appendix B in [3]). In addition, for these typical fermion masses the number of sub-halos in the corresponding WDM cosmology does not conflict with the number of Milky Way satellites [25], and is consistent with the Lyman-α forest observations [26]. The maximum entropy approach for structure formation implemented here for $\mathcal{O}(10)$ keV particles can naturally avoid the so-called 'catch-22' tension arising for fermionic halos within WDM cosmologies (based on N-body simulations, [27]). According to our approach, the fermionic density profiles allow for 'cored' like profiles in dwarfs with right sizes and masses, while being in agreement with Lyman-α bounds [10]. The results here presented open new insights in the formation and stability of DM halos. The quantum degenerate core at the center of the stable DM configurations, and its eventual core-collapse, may play a crucial role in the understanding of the formation of SMBHs in the early Universe.

The astrophysical consequences of the analysis here shown for $\mathcal{O}(10)$ keV (together with the recent results in [3, 9, 10, 17, 24]) strongly suggest that such DM *core-halo* morphology are a very plausible scenario within the late stages of non-linear structure formation.

References

[1] H. Mo, F. Van den Bosch, and S. White. *Galaxy formation and evolution*. Cambridge University Press, 2010.

[2] Hsi-Yu Schive, Ming-Hsuan Liao, Tak-Pong Woo, Shing-Kwong Wong, Tzihong Chiueh, Tom Broadhurst, and W. Y. Pauchy Hwang. Understanding the Core-Halo Relation of Quantum Wave Dark Matter from 3D Simulations. *Phys. Rev. Lett.*, 113(26):261302, December 2014.

[3] C.R. Argüelles, M.I. Díaz, A. Krut, and R. Yunis. On the formation and stability of fermionic dark matter haloes in a cosmological framework. *Mon. Not. R. Astron. Soc.*, 502(3):4227–4246, April 2021.

[4] R. Ruffini and S. Bonazzola. Systems of self-gravitating particles in general relativity and the concept of an equation of state. *Phys. Rev.*, 187:1767–1783, Nov 1969.

[5] D. Lynden-Bell. Statistical mechanics of violent relaxation in stellar systems. *Mon. Not. R. Astron. Soc.*, 136:101, January 1967.

[6] Pierre-Henri Chavanis. On the 'coarse-grained' evolution of collisionless stellar systems. *Mon. Not. R. Astron. Soc.*, 300(4):981–991, November 1998.

[7] Pierre-Henri Chavanis. Generalized thermodynamics and kinetic equations: Boltzmann, Landau, Kramers and Smoluchowski. *Physica A Statistical Mechanics and its Applications*, 332:89–122, February 2004.

[8] P.H. Chavanis, M. Lemou, and F. Méhats. Models of dark matter halos based on statistical mechanics: The fermionic King model. *Phys. Rev. D*, 92(12):123527, December 2015.

[9] C.R. Argüelles, A. Krut, J.A. Rueda, and R. Ruffini. Novel constraints on fermionic dark matter from galactic observables I: The Milky Way. *Physics of the Dark Universe*, 21:82, September 2018.

[10] C.R. Argüelles, A. Krut, J.A. Rueda, and R. Ruffini. Novel constraints on fermionic dark matter from galactic observables II: Galaxy scaling relations. *Physics of the Dark Universe*, 24:100278, March 2019.

[11] J. Katz. On the Number of Unstable Modes of an Equilibrium - Part Two. *Mon. Not. R. Astron. Soc.*, 189:817, December 1979.

[12] P.H. Chavanis and J. Sommeria. Degenerate equilibrium states of collisionless stellar systems. *Mon. Not. R. Astron. Soc.*, 296(3):569–578, May 1998.

[13] R. Ruffini, C.R. Argüelles, and J.A. Rueda. On the core-halo distribution of dark matter in galaxies. *Mon. Not. R. Astron. Soc.*, 451(1):622–628, July 2015.

[14] J.S. Bullock and M. Boylan-Kolchin. Small-Scale Challenges to the ΛCDM Paradigm. *Annu. Rev. Astron. Astrophys.*, 55(1):343–387, August 2017.

[15] R. Davé, D.N. Spergel, P.J. Steinhardt, and B.D. Wandelt. Halo Properties in Cosmological Simulations of Self-interacting Cold Dark Matter. *Astrophys. J.*, 547(2):574–589, February 2001.

[16] K. Gültekin, D.O. Richstone, K. Gebhardt, T.R. Lauer, S. Tremaine, M.C. Aller, R. Bender, A. Dressler, S.M. Faber, Alexei V. Filippenko, Richard Green, Luis C. Ho, John Kormendy, John Magorrian, Jason Pinkney, and Christos Siopis. The M-σ and M-L Relations in Galactic Bulges, and Determinations of Their Intrinsic Scatter. *Astrophys. J.*, 698(1):198–221, June 2009.

[17] E.A. Becerra-Vergara, C.R. Argüelles, A. Krut, J.A. Rueda, and R. Ruffini. Geodesic motion of S2 and G2 as a test of the fermionic dark matter nature of our Galactic core. *Astron. & Astrophys.*, 641:A34, September 2020.

[18] E.A. Becerra-Vergara, C.R. Argüelles, A. Krut, J.A. Rueda, and R. Ruffini. Hinting a dark matter nature of Sgr A* via the S-stars. *Mon. Not. R. Astron. Soc.*, 505(1):L64–L68, July 2021.

[19] S. Gillessen, P. M. Plewa, F. Widmann, S. von Fellenberg, M. Schartmann, M. Habibi, A. Jimenez Rosales, M. Bauböck, J. Dexter, F. Gao, I. Waisberg, F. Eisenhauer, O. Pfuhl, T. Ott, A. Burkert, P. T. de Zeeuw, and R. Genzel. Detection of a Drag Force in G2's Orbit: Measuring the Density of the Accretion Flow onto Sgr A* at 1000 Schwarzschild Radii. *Astrophys. J.*, 871:126, January 2019.

[20] P.M. Plewa, S. Gillessen, O. Pfuhl, F. Eisenhauer, R. Genzel, A. Burkert, J. Dexter, M. Habibi, E. George, T. Ott, I. Waisberg, and S. von Fellenberg. The Post-pericenter Evolution of the Galactic Center Source G2. *Astrophys. J.*, 840:50, May 2017.

[21] Gravity Collaboration, R. Abuter, A. Amorim, N. Anugu, M. Bauböck, M. Benisty, J. P. Berger, N. Blind, H. Bonnet, W. Brandner, A. Buron, C. Collin, F. Chapron, Y. Clénet, V. Coudé Du Foresto, P. T. de Zeeuw, C. Deen, F. Delplancke-Ströbele, R. Dembet, J. Dexter, G. Duvert, A. Eckart, F. Eisenhauer, G. Finger, N. M. Förster Schreiber, P. Fédou, P. Garcia, R. Garcia Lopez, F. Gao, E. Gendron, R. Genzel, S. Gillessen, P. Gordo, M. Habibi, X. Haubois, M. Haug, F. Haußmann, T. Henning, S. Hippler, M. Horrobin, Z. Hubert, N. Hubin, A. Jimenez Rosales, L. Jochum, K. Jocou, A. Kaufer, S. Kellner, S. Kendrew, P. Kervella, Y. Kok, M. Kulas, S. Lacour, V. Lapeyrère, B. Lazareff, J.-B. Le Bouquin, P. Léna, M. Lippa, R. Lenzen, A. Mérand, E. Müler, U. Neumann, T. Ott, L. Palanca, T. Paumard, L. Pasquini, K. Perraut, G. Perrin, O. Pfuhl, P. M. Plewa, S. Rabien, A. Ramírez, J. Ramos, C. Rau, G. Rodríguez-Coira, R.-R. Rohloff, G. Rousset, J. Sanchez-Bermudez, S. Scheithauer, M. Schöller, N. Schuler, J. Spyromilio, O. Straub, C. Straubmeier, E. Sturm, L. J. Tacconi, K. R. W. Tristram, F. Vincent, S. von Fellenberg, I. Wank, I. Waisberg, F. Widmann, E. Wieprecht, M. Wiest, E. Wiezorrek, J. Woillez, S. Yazici, D. Ziegler, and G. Zins. Detection of the gravitational redshift in the orbit of the star S2 near the Galactic centre massive black hole. *A&A*, 615:L15, July 2018.

[22] Gravity Collaboration, R. Abuter, A. Amorim, M. Bauböck, J. P. Berger, H. Bonnet, W. Brand ner, V. Cardoso, Y. Clénet, P. T. de Zeeuw, J. Dexter, A. Eckart, F. Eisenhauer, N. M. Förster Schreiber, P. Garcia, F. Gao, E. Gendron, R. Genzel, S. Gillessen, M. Habibi, X. Haubois, T. Henning, S. Hippler, M. Horrobin, A. Jiménez-Rosales, L. Jochum, L. Jocou, A. Kaufer, P. Kervella, S. Lacour, V. Lapeyrère, J. B. Le Bouquin, P. Léna, M. Nowak, T. Ott, T. Paumard, K. Perraut, G. Perrin, O. Pfuhl, G. Rodríguez-Coira, J. Shangguan, S. Scheithauer, J. Stadler, O. Straub, C. Straubmeier, E. Sturm, L. J. Tacconi, F. Vin-

cent, S. von Fellenberg, I. Waisberg, F. Widmann, E. Wieprecht, E. Wiezorrek, J. Woillez, S. Yazici, and G. Zins. Detection of the Schwarzschild precession in the orbit of the star S2 near the Galactic centre massive black hole. *A&A*, 636:L5, April 2020.

[23] T. Do, A. Hees, A. Ghez, Gregory D. Martinez, D.S. Chu, S. Jia, S. Sakai, J.R. Lu, A.K. Gautam, K.K. O'Neil, E.E. Becklin, Mark R. Morris, Keith Matthews, Shogo Nishiyama, Randy Campbell, Samantha Chappell, Zhuo Chen, Anna Ciurlo, Arezu Dehghanfar, Eulalia Gallego-Cano, Wolfgang E. Kerzendorf, James E. Lyke, Smadar Naoz, Hiromi Saida, Rainer Schödel, Masaaki Takahashi, Yohsuke Takamori, Gunther Witzel, and Peter Wizinowich. Relativistic redshift of the star S0-2 orbiting the Galactic Center supermassive black hole. *Science*, 365(6454):664–668, August 2019.

[24] C.R. Argüelles et al. What does lie at the Milky Way centre? Insights from the s2-star orbit precession. *Mon. Not. R. Astron. Soc.*, 511(1):L35–L39, March 2022.

[25] E.J. Tollerud, J.S. Bullock, L.E. Strigari, and B. Willman. Hundreds of Milky Way Satellites? Luminosity Bias in the Satellite Luminosity Function. *Astrophys. J.*, 688(1):277–289, November 2008.

[26] V. Iršič, M. Viel, M.G. Haehnelt, J.S. Bolton, S. Cristiani, G.D. Becker, V. D'Odorico, G. Cupani, Tae-Sun Kim, Trystyn A.M. Berg, S. López, S. Ellison, L. Christensen, K.D. Denney, and G. Worseck. New constraints on the free-streaming of warm dark matter from intermediate and small scale Lyman-α forest data. *Phys. Rev. D*, 96(2):023522, July 2017.

[27] A.V. Macciò, S. Paduroiu, D. Anderhalden, A. Schneider, and B. Moore. Cores in warm dark matter haloes: a Catch 22 problem. *Mon. Not. R. Astron. Soc.*, 424(2):1105–1112, August 2012.